Performance Analysis of a Residential Wind-Turbine Dual-Stator Winding Synchronous Reluctance Generator with Armature Reaction Effect

Thuso Karen Mulelu and Mbika Muteba, *IEEE Member*
Department of Electrical and Electronic Engineering Technology, University of Johannesburg,
PO Box 17011, Doornfontein 2028, Johannesburg, South Africa
karen.mulelu@gmail.com; mmuteba@uj.ac.za

***Abstract*—The electric generators in residential wind-turbine drivetrains do not only require high ratio power per mass, high efficiency and good overload capabilities, but they also require less volume and quick dynamic responses during severe loading, start-ups, shut-downs and during emergency stops. This paper deals with the analysis of a three-phase dual stator-winding synchronous reluctance generator (DSWSynRG) for residential wind-turbine drivetrains. The performance of the DSWSynRG is evaluated by means of 2D Finite Element Analysis (FEA), and the armature reaction effects are accounted for in the analysis of the generator performance parameters. The stator of the DSWSynRG has two magnetically coupled three-phase windings (main and auxiliary), distributed in 36 slots. The auxiliary (excitation) winding provides the most needed *q*-axis magnetic flux for voltage generation in the main (armature) winding. The DSWSynRG has rated and peak powers of 5.5 kW and 7 kW respectively. From the FEA results, it is evident that the armature reaction has a magnetizing effect for both resistive and inductive load. The results also evidenced that the effect of armature reaction is more distortional for inductive than resistive load.**

Keywords—Dual stator winding, residential wind turbine, Synchronous reluctance generator, armature reaction.

I. INTRODUCTION

Electrical power generation from wind turbine drivetrains has rapidly developed in recent years [1-2] and recent conservative estimations indicate a steady growth of the small-scale wind turbines market [3]. The capacity for small scale wind turbines is generally regarded as from 1 kW to 100 kW. The DSWSynRG analyzed in this paper is more suitable in residential small-scale wind turbine drivetrains due to less system weight and volume. The concept of dual-stator winding is not new at all. In more than three decades, the concept has been proposed to enhance the power factor of three-phase induction motors [4-5]. Very recently, a three-phase asynchronous generator having the concept of dual stator winding, and feeding loads that require variable frequency generating system in large aircrafts has been reported [6]. In 2014, the three-phase induction generator with dual stator winding was studied for parameter design and static performance for ac generating system with inductive and capacitive loads [7]. In [8] and [9] the three-phase induction generator with dual stator winding was analyzed for standalone small electric power plant to feed isolated loads.

The poor power factor due low saliency ratio in three-phase synchronous reluctance machine with simple salient pole rotor has motivated the use of auxiliary capacitive winding to improve the power factor. The dynamic and transient behaviors line-start synchronous reluctance machine having a salient rotor type, with a magnetically coupled three-phase stator auxiliary windings and reactive compensation is analyzed in [10]. The analysis and performance characterization of the dual-winding salient-pole synchronous reluctance generator fed with direct current control winding excitation is reported in [11]. In the later the auxiliary winding is fed with a dc source, and the frequency of the generated voltage is directly related to the rotor speed. On the other hand the load voltage is regulated by optimal selection of the excitation capacitors [11]. Although saturation effect, core and harmonic losses were included in the dynamic and steady state models of the generator feeding either an impedance or a rectifier load in the work presented in [11], the effect of armature reaction were left out in the analysis.

In addition to the above, the results in the work reported in [10] evidenced that the use of auxiliary capacitive winding improved tremendously the power factor; the results also proved that the electromagnetic torque is enhanced by the capacitive compensation. However, the system weigh of the rotor is greatly reduced when the rotor of a synchronous reluctance machine is a transverse-laminated type and having a certain number of air-barriers per pole, which is not also the case for the generator model reported in [11].

The rotor with multiple air-barriers gives the synchronous reluctance machine the capability to respond very quickly to dynamic changes especially in wind turbine drivetrain applications. Therefore, this paper analyses the performance of a DSWSynRG having four flux barriers per pole, taking into account the effect armature reaction for both resistive and inductive load currents.

II. Specifications and Ratings

Fig.1 (a) shows the sketch of DSSynRG with direct capacitance injection for a typical residential wind turbine drive train, while Fig.1 (b) illustrates a pole of the cross section of the DSWSynRG.

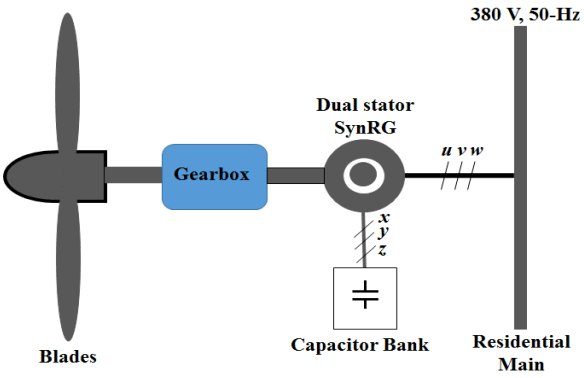

(a)

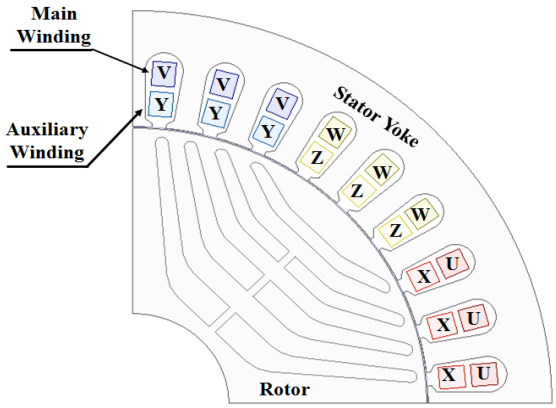

(b)

Fig. 1. (a) DSSynRG with direct capacitance injection (a) a pole of the cross section of the DSWSynRG,

The dual-stator synchronous reluctance generator analysed in this paper has a rated speed of 1500 rpm with base frequency of 50-Hz. The generator is designed for rated power, current and voltage of 5.5 kW, 12.97 A and 380 V respectively. The rotor has flux barriers, three radial magnetic ribs and eight tangential magnetic bridges per pole. The *d*-and *q*-axis magnetizing inductances are found to be 3.8664 H and 1.906 H respectively, giving a saliency ratio of 2.03.

III. Dynamic Model of the DSWSynRG

The wind turbine model that describes the dynamic's behavior of the machine, which depends on the interaction between the wind and the rotor, also known as aerodynamic model is presented in [12] and [13]. The dynamic's behaviour pertained to the aerodynamic model as elaborated in [12] and [13], are not discussed in this paper. However, this paper presents the dynamic model that describes the mechanical equations of DSWSynRG for no-load and full load operations, in the wind turbine drivetrain system. It is noted that the following assumptions are observed in the dynamic model:

- Both armature and excitation windings are to be sinusoidally distributed along the airgap.
- Saturation is not considered.

The voltage equations that describe the electrical characteristics of the DSSynRG in machine variables *uvw* and *xyz* are given as in (1) and (2) respectively.

$$V_{uvw_s} = -r_{uvw_s} i_{uvw_s} - \frac{d}{dt}\lambda_{uvw_s} \tag{1}$$

$$0 = r_{xyz_s} i_{xyz_s} + \frac{d}{dt}\lambda_{xyz_s} + Vc_{xyz_s} \tag{2}$$

Here the subscript *s* denote the variables associated with the stator, while *uvw* and *xyz* represent the armature and the excitation windings respectively. The resistances r_{uvws} and r_{xyzs} are diagonal matrices, and the flux linkages for the armature and excitation windings are given as in (3) and (4) respectively.

$$\lambda_{uvw_s} = L_{uvw_s} I_{uvw_s} + L_{uvwxyz_s} I_{xyz_s} \tag{3}$$

$$\lambda_{xyz_s} = L_{xyzuvw_s} I_{uvw_s} + L_{xyz_s} I_{xyz_s} \tag{4}$$

Where L_{uvws} and L_{xyzs} are the self and mutual inductances of the armature and excitation windings respectively. On the other hand, L_{uvwxyz} and L_{xyzuvw} are the coupling inductances between the two windings. Fig.2 shows the *dq* equivalent circuit of a dual stator winding DSSynRG with direct capacitance injection.

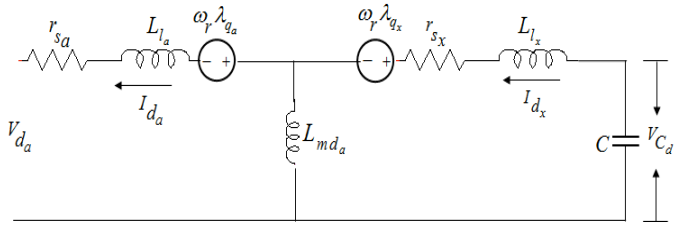

(a)

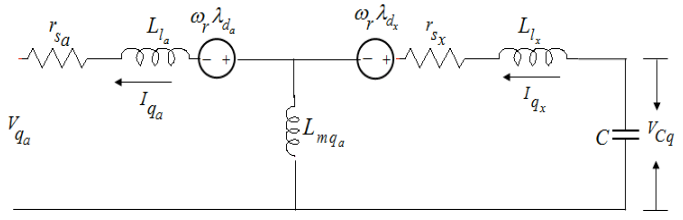

(b)

Fig. 2: *dq* equivalent circuits, (a) *d*-axis, (b) *q*-axis

The voltage equations that describe the electrical characteristic of the DSSynRG, in rotating reference frame are given by

$$V^r_{qds_a} = -r_{s_a} i^r_{qds} - \overline{\omega}\lambda^r_{qd_{sa}} - \frac{d}{dt}\lambda^r_{qd_{sa}} \tag{5}$$

$$0 = r_{s_x} i^r_{qds_x} + \overline{\omega}\lambda^r_{qds_x} + \frac{d}{dt}\lambda^r_{qds_x} + V^r_{Cqds_x} \tag{6}$$

Here the superscript *r* represents the rotor reference frame, and subscripts *a* and *x* refer to the armature and excitation windings respectively. On no-load the three-phase armature (main) windings do not carry any current. With direct capacitance injection into the auxiliary winding, a reluctance torque is developed on no-load, which is due to excitation current, and the electromagnetic torque on no-load is given as

$$T_{elm} = \left(\frac{3}{2}\right)\left(\frac{p}{2}\right)[(L_{d_x} - L_{q_x}) I^r_{d_x} I^r_{q_x}] \tag{7}$$

On load the three-phase armature (main) windings carry stator currents which develop a second reluctance torque due to load current and capacitance attached to it. The interaction between the currents flowing in armature and excitation windings develop a third reluctance torque. The later can be seen as a reaction torque. In the absence of direct capacitance injection, the DSWSynRG will not develop any power on no-load. On other hand, the residual magnetic flux will not be able to contribute to voltage build up in case where a load is connected to the armature winding. The necessity of having permanent and direct capacitance injection into the exciting winding is needed. The electromagnetic torque developed by the DSSynRG on load is given by (8). Observing (8), it is noted that the electromagnetic torque has three components. The first is due to the no-load excitation current, while the second is and third terms are due to armature reaction.

$$\begin{aligned} T_{elm} = \left(\frac{3}{2}\right)\left(\frac{p}{2}\right)[&(L_{das} - L_{qas}) I^r_{das} I^r_{qas} \\ &+ (L_{dxs} - L_{qxs}) I^r_{dxs} I^r_{qxs} \\ &+ (L_{mdas} - L_{mqas})(I^r_{qas} I^r_{dxs} + I^r_{das} I^r_{qxs})] \end{aligned} \tag{8}$$

The typical wind turbine drivetrain mechanical equation used for simulation is well elaborated in [14]. In this paper, the friction coefficient is ignored and the dynamic equation of the DSWSynRG is given by

$$\frac{2J}{p}\frac{d\omega_r}{dt} = T_m - T_{elm} - T_w \tag{9}$$

Expending (7) and (9), the mechanical equation that describes the dual stator winding synchronous reluctance generator dynamic model on no-load, in rotating reference frame is given by

$$\frac{d\omega_r}{dt} = \frac{p}{2J}(T_m - T_w) - \frac{3p^2}{8J}[(L_{ds_x} + L_{qs_x}) I^r_{ds_x} I^r_{qs_x}] \tag{10}$$

Here J is the total inertia of the rotor, T_m is input mechanical torque and T_w is the load torque of the wind turbine. The mechanical equation that describes the dual stator winding synchronous reluctance generator dynamic model on load, in rotating reference frame is obtained by expending (8) and (9), and it is given as

$$\begin{aligned} \frac{d\omega_r}{dt} = \frac{p}{2J}(T_m - T_w) - \frac{3p^2}{8J}[&(L_{ds_a} + L_{qs_a}) I^r_{ds_a} I^r_{qs_a} \\ &+ (L_{ds_x} + L_{qs_x}) I^r_{ds_x} I^r_{qs_x} \\ &+ (L_{mds_a} + L_{mq_{sa}})(I^r_{ds_x} I^r_{qs_a} + I^r_{ds_a} I^r_{qs_x})] \end{aligned} \tag{11}$$

The effect of armature reaction has an impact on the power developed. In addition to the electromagnetic power due to excitation and load current, there is also a reaction power that has been developed, which is due to reaction torque.

IV. Finite Element Analysis

A. Effect of armature reaction on the flux density distribution

The cross section of a single pole for the DSWSynRG is shown in Fig. 1 (b). The auxiliary (excitation) winding is designed to carry a small excitation capacitive current, while the main (armature) winding is destined to generate voltage for load current rated up to 12.97 A. To study the effect armature reaction on performance parameters of the DSWSynRG, the 2D FEA is used for ac magnetic transient solution. The load current space vector angle is set at 20^o electric. The resistive or inductive full-load *d*-and *q*-axis currents are 12.178 A and 4.432 A respectively. Fig.3 to Fig.5 show the flux-density distributions for different loading conditions with the DSWSynRG driven at 1500 rpm for *q*-axis excitation currents of 7.778 A and 3.89 A respectively.

From Fig 3 to Fig.5, it is well observed that tangential and radial magnetic ribs are heavily saturated by the *q*-axis flux density set up by the excitation *q*-axis current. The influence of armature reaction due to load current is clearly noticeable in the flux-density distribution. Observing the FEA results, it is noted that the load current increases the stator back iron localized flux density from ± 1.5 Tesla for no-load operation up to ± 2 Tesla and 2.5 Tesla for resistive and inductive full-load operations respectively, with *q*-axis excitation current of 7.778 A . The localized saturation of stator back iron, the heavy saturation of tangential and radial magnetic ribs are more visible for inductive than resistive load. This informs that the load currents have an impact on the magnitude of the airgap flux density harmonic components.

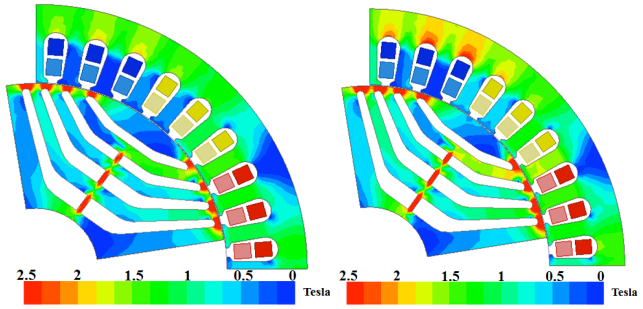

(a) (b)

Fig. 3. Flux-density distribution on no-loat (a) q-axis excitation of 3.89 A a(b) *q*-axis excitation of 7.778 A

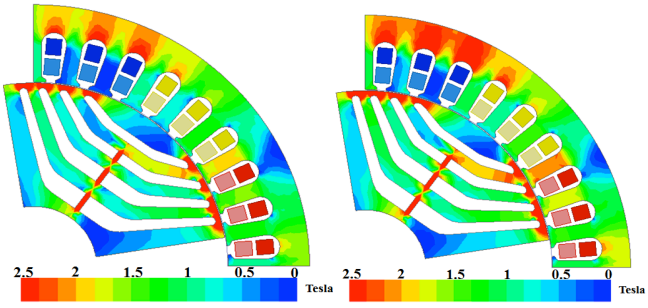

(a) (b)

Fig. 4. Flux-density distribution at resistive full-load (a) *q*-axis excitation of 3.89 A, (b) *q*-axis excitation of 7.778 A at resistive full-load

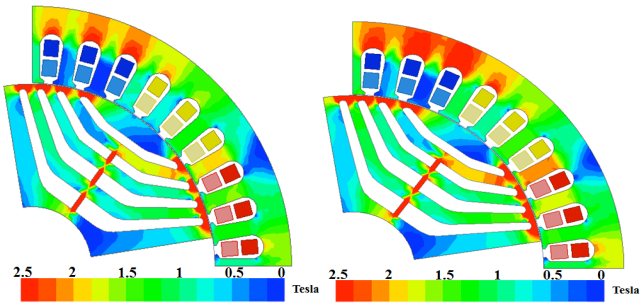

(a) (b)

Fig. 5. Flux-density distribution at inductive full-load (a) *q*-axis excitation of 3.89 A, (b) *q*-axis excitation of 7.778 A at resistive full-load

B. Effect of armature reaction on the induced voltage, developed torque and delivered power

The induce voltage profiles are shown in Figs 6 (a) to (c), while the FFTs of the profiles are illustrated in Fig 6 (d). In addition to the stator winding configuration and stator slotting, the quality of the induced voltage waveforms is also influenced by armature reaction. Owing to the latter, it is well reported in [15] that voltage distortion is also due to nonlinear loads connected to the network.

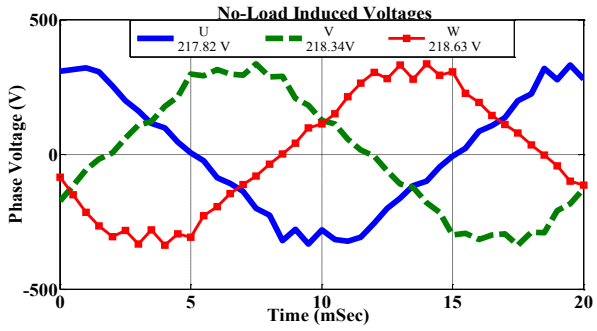

(a)

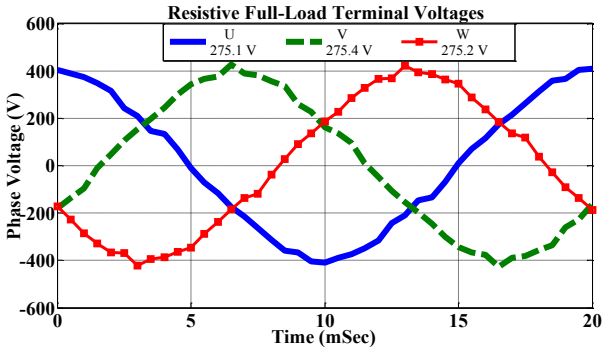

(b)

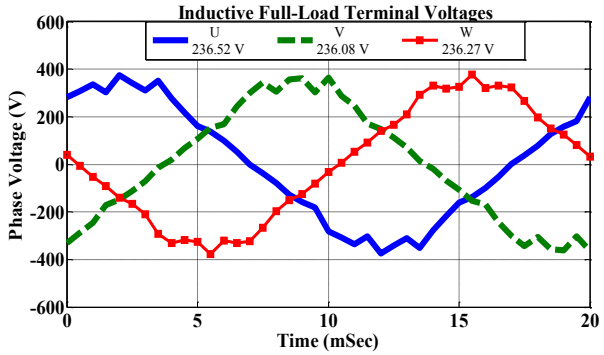

(c)

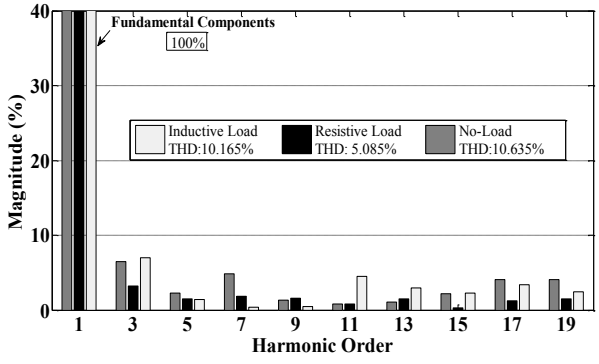

(d)

Fig. 6. Induced Voltage at 1500 rpm, 200µF (a) No-load (b) Resistive Full-load, (c) Inductive Full-load, (d) Comparison of induced voltages harmonic contents

Observing the FFTs results in Fig 6 (d), it is evident that the first and second stator winding phase belt harmonics (5^{th} and 7^{th}) and the first and second stator slot harmonics (17^{th} and 19^{th}) are dominent under no-load operation, and strongly contribute to its high THD of 10.635 %. Under full load operation, the rms value of the phase voltage increses from ± 218 V on no-load to ± 236 V and ± 275 V inductive and resistive full-load respectively. This is due to magnetizing effect of armature reaction. The fundamental component of the induced voltage is high for resistive load than inductive load, thus increasing the root means square value when the DSWSynRG operates with a resistive load.

Under inductive full-load operation, the second stator phase belt harmonic (7^{th}) has dropped tremendously, but the 3^{rd} harmonic contents due saturation and the 11^{th} rotor slot harmonics are still dominant, keeping the THD at 10.165 %. On the other hand, the THD computed for resistive load stands low at 5.085 % due the minimization of mainly the 7^{th}, 17^{th} and 19^{th} harmonic components. The effect of armature reaction for inductive load is more distortional than magnetizing, while the effect is more magnetizing for resistive load than distortional. The typical residential home has power tool loads such as washing machine, dish washer, hand drier, refrigerator etc. These loads are highly inductive are will contribute to the distortion of voltage and current. On other hand, light bulbs, geysers, stoves, irons etc., which are more resistive, will contribute to the magnetizing effect.

Fig 7 (a) shows the Instantanous Electromagntic torque for no-load and resistive full-load operation, while Fig 7 (b) illustrates the steady-state delivered active power as a function of current vector angle.

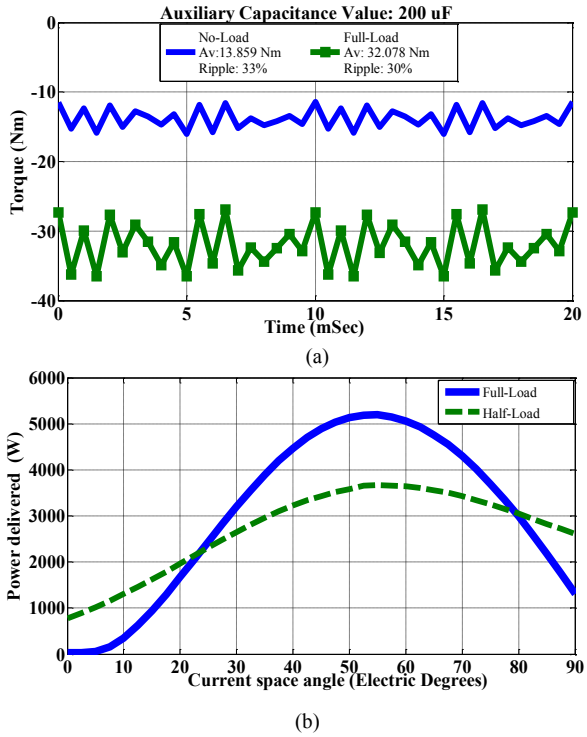

Fig. 7. (a) Instantanous Electromagntic torque , (b) Steady-state delivered active power

Observing Fig 7 (b), it is noted that from 0^o to 20^o *elect* and from 80^o to 90^o *elect*, the DSWSynRG delivered more active power at half-load. There is less magnetizing effect for half-load operation, thus the voltage induced on half-load is less than the voltage induced on full-load. For same input wind turbine torque, the current space angle should be adjusted such that the DSWSynRG delivers active power having a magnitude that is dependent on the load impedance.

III. CONCLUSION

In this paper, the performance of a dual stator winding synchronous reluctance generator for a residential wind turbine drivetrain has been analyzed, taking into account the effect of armature reaction. From the FEA results, it was noted that the saturation of the magnetic bridges did not only increase the fundamental airgap flux density , but it also increased some of the components of the airgap flux density. It is therefore noted that the effect of armature reaction in both resistive and inductive load is magnetizing. The magnitude of the magnetization effect depends also on the power factor. The effect is more magnetizing for lagging power factor than unity power factor. However, the fundamental airgap flux density is greater for a resistive load (unity power factor) as compare to the inductive load (lagging power factor). On the other hand, the THDs of the airgap flux density is high for inductive load as compare to resistive load. The effect of armature reaction for inductive load is more distortional than magnetizing, while the effect is more magnetizing for resistive load than distortional.

REFERENCES

[1] C. Haidar, R. Boutarfa, S. Harmand, "Fluid Flow and Convective Heat Transfer Analysis on a Rotor of Wind Turbine Alternator with an Impinging", International Journal of Renewable Energy, Vol.9, No. 3, September 2019. pp.1144-1153

[2] A Harrouz, I. Colak, and Korhan Kayisli, "Control of a Small Wind Turbine System Application", 5^{th} International Conference on Renewable Energy Research and Applications, Nov 20-23, 2016, pp. 1128-1133, Birmingham, UK.

[3] J. C. Mitchell ; M. J. Kamper ; C. M. Hackl, Small-Scale Reluctance Synchronous Generator Variable Speed Wind Turbine System with DC Transmission Linked Inverters, 2016 IEEE Energy Conversion Congress and Exposition (ECCE)

[4] N. Bianchi, S. Bolognani, F.Tonel Thermal Analysis of a Run-Capacitor Single-Phase Induction Motor. IEEE Trans Ind Appl. pp. 457-465.2003

[5] Wu Hanguang, Chen XIUMIN, Lu Xianliang and You Linjuan."An Investigation on Three-Phase Capacitor Induction Motor", Proceedings of Third Chinese International Conference on Electrical Machines. Aug 29-31, 1999. Xi'an, China, pp 87-90

[6] M. Muteba, "Performance Evaluation of a Dual Stator-Winding Three-Phase Asynchronous Generator with Armature Reaction Effect", IEEE Transportation Electrification Conference and Expo (ITEC), June 19-21, 2019, NOVI, MI, USA.

[7] F. Bu, Y. Hu, W. Huang and S. Zhuang, "Parameter Design and Static Performance of Dual Stator-Winding Induction Generator Variable Frequency AC Generating System with Inductive and Capacitive Load", IEEE Trans on Industrial Electronics, Vol.61, No.8, August. 2014. pp. 3902-3914

[8] D. Fodorean, L. Szabo and A. Miraoui, " Generator Solutions for Stand Alone Pico-Electric Power Plant", IEEE International Electric Machines and Drives Conference, May 3-6, 2017, Miami, FL, USA

[9] M. Faisal Khan and M. Rizwan Khan, " Voltage control of Single-Phase Two Winding Self-Excited Induction Generator for Isolated Loads", International Conference on Advances in Energy Conversion Technologies (ICAECT), Jan 23-25, 2014, Manipal, India.

[10] A. S. O. Ogunjuyigbe, A. A. Jimoh and T.R. Ayodele, " Dynamic and transient behavior of a line start, capacitance compensated synchronous reluctance machine" Journal of Electrical Systems and Information Technology, Vol. 4, Is.3, pp. 843-860, Dec. 2018.

[11] O. Ojo, A. Ginart, O. Omozusi, and A. A. Jimoh, "Synchronous operation of a dual-winding reluctance generator" IEEE Trans on Energy Conv. Vol. 12. No.4, 1997, pp. 357-362. 1997.

[12] M. Tahiri, A. Djebli and A. Mimet, "Drivetrain Flexibility Effect on Control Performance of a Horizontal Axis Wind Turbine", International Journal of Applied Engineering Research, Vol.12, No.16, pp.5511-5519, 2017.

[13] A.G. Abo-Khalil, "Grid Connection Control of DFIG in Variavle Speed Wind Turbines under Turbulent Conditions", International Journal of Renewable Energy, Vol.9, No. 3, September 2019.

[14] K. E. Okedu, "Effects of Drive Train Model Parameters on a Variable Speed Wind Turbine", International Journal of Renewable Energy, Vol.2, No. 1, 2012, pp. 92-98.

[15] J. Hussain, M. Hussain, S. Raza and M. Siddique, "Power Quality Improvement of Grid-Connected Wind Energy System Using DSTATCOM-BESS", International Journal of Renewable Energy, Vol.9, No. 3, PP. 1388-1397, September 2019.